

Comparative Study between Common and Individual MPPT Controller Using Fuzzy Logic Control for Hybrid System (Photovoltaic/Wind Energy Conversion System)

Zahira Bouguerra^{1*}

¹ Department of Electromechanical Engineering, Faculty of Sciences and Technologies, University of Mohamed El Bachir El Ibrahimy, 34030 Bordj Bou Arreridj El-Anasser, P.O.B. 64, Algeria

* Corresponding author, e-mail: zahira.bouguerra@univ-bba.dz

Received: 09 August 2024, Accepted: 23 December 2024, Published online: 23 January 2025

Abstract

This paper aims to hybridize photovoltaic systems (PVs) with wind energy conversion systems (WECs) by using different architectures, with a comparative study to distinguish the best hybridization method that gives the best performance. The first architecture uses an individual maximum power point tracking (MPPT) controller for each system independently. The photovoltaic generator is connected to the DC/DC converter and is controlled by fuzzy logic control (FLC) to track maximum power. In the WECs system, which is based on a permanent magnet synchronous generator (PMSG), the DC/DC converter is also controlled by FLC to maximize its output power. The second architecture uses a single MPPT controller for both systems; the PV generator and AC/DC converter of the WECs are connected to a common DC/DC converter controlled by the FLC. The hybrid system is connected to the grid via an inverter, which is controlled by voltage-oriented control (VOC) to separate the control of the active and reactive powers. The system studied was specially designed to be installed in the building, consisting of a photovoltaic system providing 25 kW and a WECs composed of three small turbines, each providing 8.5 kW. The MATLAB simulation results are presented under varying conditions of sunlight, wind speed, and load requirement, proving that; the using of an individual MPPT controller gives better performances than the single MPPT controller. However, the last topology provides more power than the first topology (over 1 kW) because of the reduced number of converters used.

Keywords

PVs, WECs, MPPT, PMSG, fuzzy logic control, voltage-oriented control

1 Introduction

The growth of the human population has resulted in a significant increase in energy demand [1]. Oil, coal, and natural gas are mainly used to produce electricity. However, these traditional energy sources have dangerous effects on the environmental balance and human health, such as CO₂ emissions, pollution, and climate change. These latter risks force the world to use renewable energy to ensure a suitable future, offering many advantages over conventional power generation systems, such as environmental safety, reliability, and abundant presence. In recent decades, the fraction of renewable energy in the world energy consumption is continuously increasing at a high rate and becoming a significant energy resource of the world [2].

Generally, wind energy and photovoltaic energy are complementary because a sunny day is often calm, and the

wind is either strong on a cold day or at night. Therefore, the integration of these two sources to form a hybrid system (wind energy conversion systems (WECs)/photovoltaic systems (PVs)) is an excellent option for the production of energy with better performance than individual sources. In cities where buildings are connected to the grid, the grid plays a dual role: a storage system when the power produced is higher than the power demanded and a power supplier when the hybrid system is unable to satisfy the demand. Since converter control is an important step in matching the system voltage and current to the grid and increasing the total system efficiency, the hybridization topology also plays a crucial role in hybrid systems that can influence system efficiency.

Different topologies are utilized in literature for the hybridization of these two systems (PVs and WECs) with

different controls; in [3], a single maximum power point tracking (MPPT) controller based on neural network (NN) methods are used to control PVs and WECs systems simultaneously. In [4] and [5] each renewable source is connected to the grid by its individual DC/DC and DC/AC converters controlled by NN and fuzzy logic control (FLC). In [6–9], each system is controlled separately by its MPPT (FLC) and connected to a common inverter. However, the differences between these structures remain unclear. Therefore, a comparative study between two topologies of hybridization (a common MPPT and an individual MPPT) is detailed in this work.

This study is interested in making a comparison study between two topologies of PVs/WECs hybridization.

The first uses the individual MPPT controllers for each subsystem. In the second topology, a common MPPT control is applied to minimize the converters utilized and minimize the loss of power presented. For this purpose, the paper is organized as follows; the second part details the modeling of different components and controls of this system. In Section 5, the simulation results of both topologies and their comparisons are presented.

2 System description

Fig. 1 shows two topologies of hybridization studied in this work that combine the PV and WEC systems; the first is based on connecting both systems to a DC bus through two separate DC/DC converters that apply individual

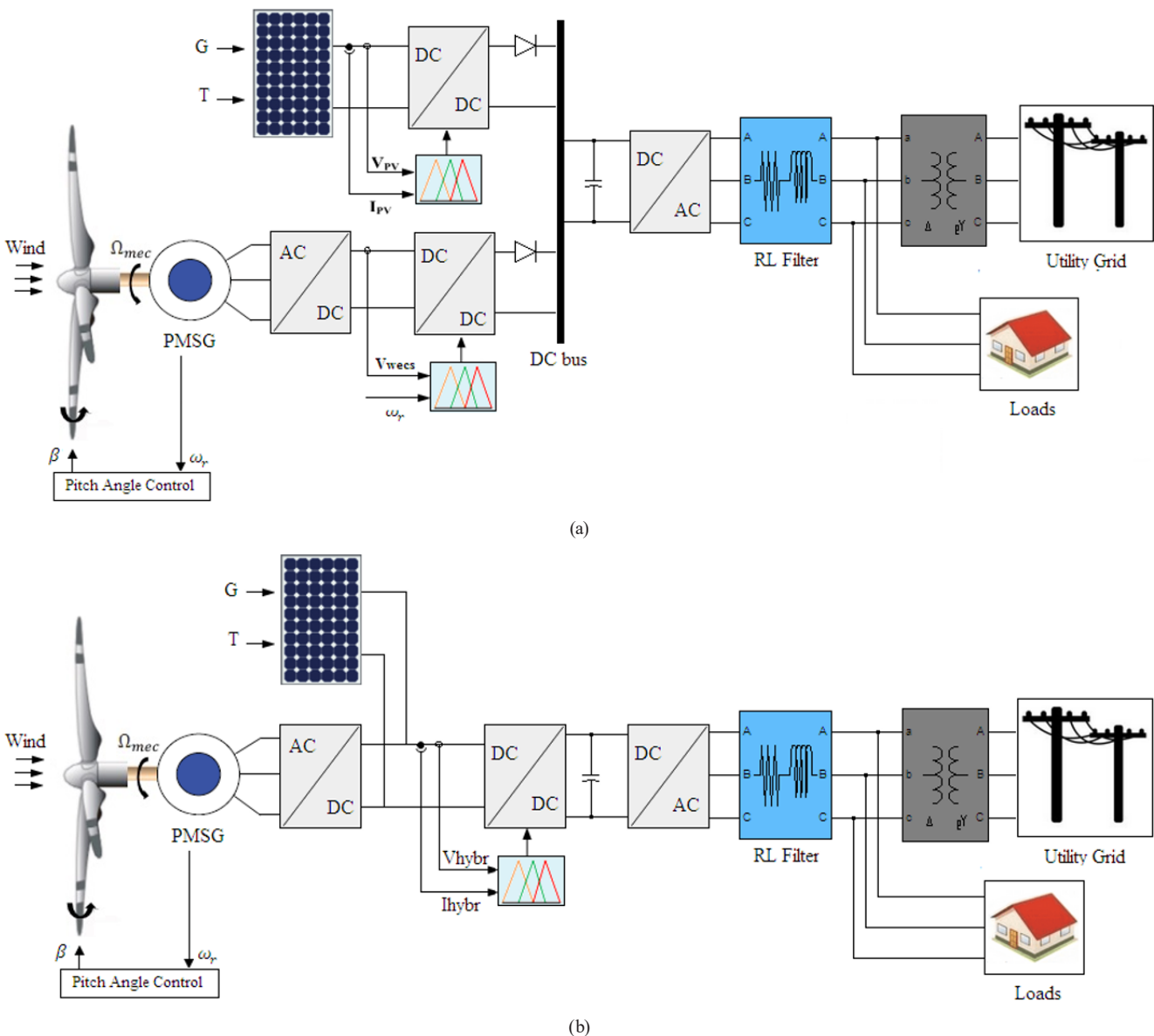


Fig. 1 Hybridization Topologies: (a) individuals MPPT, (b) common MPPT

MPPT control. The second is based on connecting both systems to a common DC/DC converter by applying a common MPPT controller.

3 System modeling

3.1 PV generator

A photovoltaic cell is a semiconductor diode that converts irradiation into electricity through the photovoltaic effect. Various models were utilized to represent the highly non-linear behavior of the semiconductor junction under variable solar radiation and temperature [10]. Among them, the single diode is the most used due to its simplicity and high performance. The circuit is shown in Fig. 2.

Because a typical PV cell produces approximately 2 W, the cells have to be connected in a series-parallel connection to produce enough power [11]. As a result, combining modules in series and parallel can build a PV array that delivers the required power. Grouping modules in series increases the output voltage of the photovoltaic generator, and grouping them in parallel increases the current. Photovoltaic currents are detailed in Eq. (1):

$$\left\{ \begin{array}{l} I_{PV} = I_{ph}N_p - I_oN_p \left[\exp\left(\frac{V_{PV} + R_s I_{PV}}{aKT N_s}\right) - 1 \right] - \frac{V_{PV} + R_s I_{PV}}{R_p N_s} \\ I_{ph} = \left[I_{sc} + K_i(T - T_{ref}) \right] \frac{G}{G_{ref}} \\ I_o = I_{o,n} \left(\frac{T}{T_{ref}} \right)^3 \exp\left[\frac{qE_g}{aK} \left(\frac{1}{T_{ref}} - \frac{1}{T} \right) \right] \\ I_{o,n} = \frac{I_{sc}}{\left[\exp\left(\frac{qV_{oc,n}}{nKT}\right) - 1 \right]} \end{array} \right. , \quad (1)$$

where I_{ph} is the photo-current, N_s is the number of cells in series, N_p is the number of cells in parallel, I_o is the saturation current, R_s is the series resistance, R_p is the parallel resistance, a is the ideality factor, E_g is the band gap voltage.

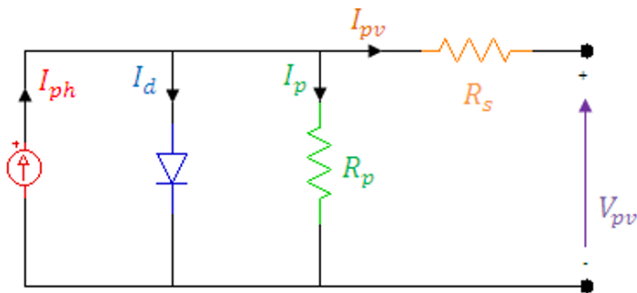


Fig. 2 Solar cell

As the PV equation shows, the output current varies as a function of solar irradiation and temperature, which immediately causes the output power to vary, which is proportionally related to it ($P_{PV} = I_{PV} \times V_{PV}$). From Fig. 3, at each irradiation value, the PV output has a peak point that presents the maximum output power ($P_{max} = I_{max} \times V_{max}$) that the PV module can produce. Therefore, a MPPT controller is required to track this peak point according to different variations in irradiance, by controlling the duty cycle of the DC/DC converter that connects the PV modules to the inverter. In general, it is based on the variation of the duty cycle according to the evolution of its input parameters (I and V) until the generator reaches its optimum operating value regardless of instabilities.

3.2 Wind turbine modeling

The wind forces turn the turbine blades that induce a shaft rotation. The permanent magnet synchronous generator (PMSG) converts this mechanical rotation to electrical power [6]. According to the Betz theorem, the maximum energy recoverable from the wind by the rotor is around 59% of the total wind energy. The aerodynamic power is then equal to the wind energy multiplied by a power factor that characterizes the turbine. This aerodynamic power is given in Eq. (2) [12]:

$$P_{aer} = \frac{1}{2} \rho \pi R^2 C_p(\lambda, \beta) v^3. \quad (2)$$

In the WEC system, the output power is affected by geographical and metrological conditions [13]. This power is directly related to the wind speed which causes it to fluctuate as the wind changes. It is also related to the power coefficient C_p which depends strongly on the blade

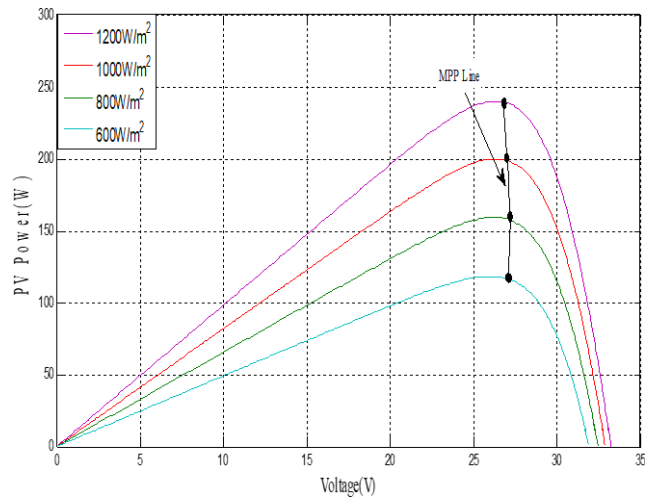


Fig. 3 PV characteristics

pitch angle β and the tip speed ratio λ , as shown in the following function [14]:

$$C_p(\lambda, \beta) = 0.5176 \left(\frac{116}{\lambda_i} - 0.4\beta - 5 \right) e^{\frac{-21}{\lambda_i}} + 0.0068, \quad (3)$$

$$\begin{cases} \frac{1}{\lambda_i} = \frac{1}{\lambda + 0.08\beta} - \frac{0.035}{\beta^3 + 1} \\ \lambda = \frac{R \times \omega_r}{V_w} \end{cases}, \quad (4)$$

where ρ is the air density, R is the radius of the turbine blades, ω_r is the rotor mechanical speed of the turbine.

The mechanical equation of the rotating parts is given by [15]:

$$\frac{d\omega_r}{dt} = \frac{1}{J} (T_{aer} - T_{em} - T_d), \quad (5)$$

where J is the total equivalent inertia of the turbine and generator, T_{aer} is the aerodynamic torque ($T_{aer} = P_t/\omega_r$), $T_d = k_r \omega_r$, k_r is the viscous friction coefficient of PMSG.

3.3 PMSG model

Owing to its simple structure, availability, reliability, and efficient power generation capability, the PMSG-based wind turbine is generally preferred [16]. Moreover, the PMSG includes a permanent magnet rather than an excitation winding, which results in a smaller pole pitch and compatibility with low-speed applications [17]. The PMSG model in dq -reference is given in Eq. (6) [18]:

$$\begin{cases} V_{sd} = R_s I_{sd} + L_d \frac{d}{dt} I_{sd} - \omega_e L_q I_{sq} \\ V_{sq} = R_s I_{sq} + L_d \frac{d}{dt} I_{sq} + \omega_e L_d I_{sd} + \omega_e \Phi_f \end{cases}. \quad (6)$$

The electromagnetic torque is given in the following function [19]:

$$T_{em} = \frac{3}{2} p [\phi_e I_q + (L_d - L_q) I_d I_q]. \quad (7)$$

If the permanent magnet is mounted on the rotor surface, then L_d becomes equal to L_q [20]. Consequently:

$$T_{em} = \frac{3}{2} p \phi_e I_q, \quad (8)$$

where V_d , V_q and I_d , I_q are respectively the stator voltages and currents in (d,q) reference, L_d , L_q are the dq axis inductances, R_s is the stator resistance, Φ_f is the permanent magnetic flux, ω_e is the PMSG electrical rotating speed ($\omega_e = p\omega_r$), and p is the number of poles.

3.4 Pitch angle control

To guarantee wind turbine system protection and safety, and maintain the power at its rated value, a mechanical technique called the pitch angle control is usually used to adjust the pitch angle of the blades according to the wind speed [21]. As shown in Fig. 4, the power coefficient is strongly dependent on the pitch angle β , whose variation changes gradually the C_p value. As a result, the aerodynamic power changes as it has a linear relationship with it.

The pitch-angle system is used to adjust the orientation of the blades according to wind speed, thus varying the power coefficient to obtain maximum output. The pitch actuator is a nonlinear servo that generally rotates all of the blades or a part of them [22]. At high wind speeds, this system can stop the turbine from operating for safety reasons. To achieve this control, three DC motors are installed on each blade, controlled by fuzzy logic to adjust the pitch angle of each blade independently according to the wind speed available in its direction, as illustrated in Fig. 5.

3.5 MPPT control

Due to the change in photovoltaic and wind power outputs with weather variations (irradiance, wind speed), some methods are used to operate these systems near their maximum point. The FLC can decompose an unknown, complex, and nonlinear system into several subsystems based on human information about the system using membership functions and fuzzy rules, which results in very satisfactory performance, high efficiency, and robustness. The FLC controller varies the duty cycle of the DC/DC converter to attain the voltage corresponding to the maximum power despite weather variations. The error and

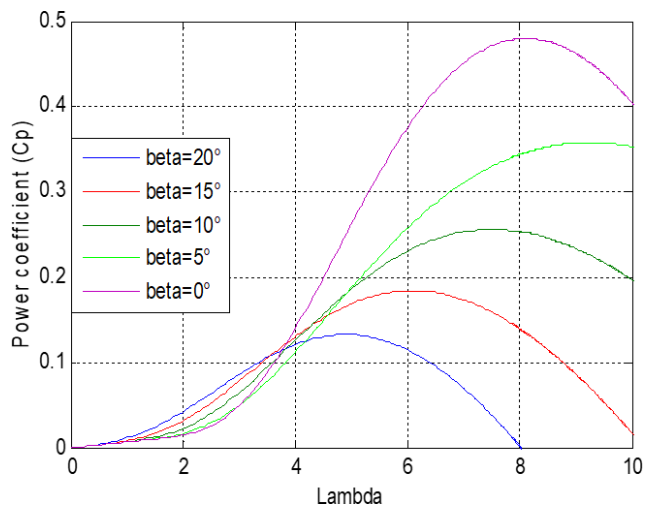


Fig. 4 Characteristic curves $C_p(\lambda)$ (β , expressed in degree)

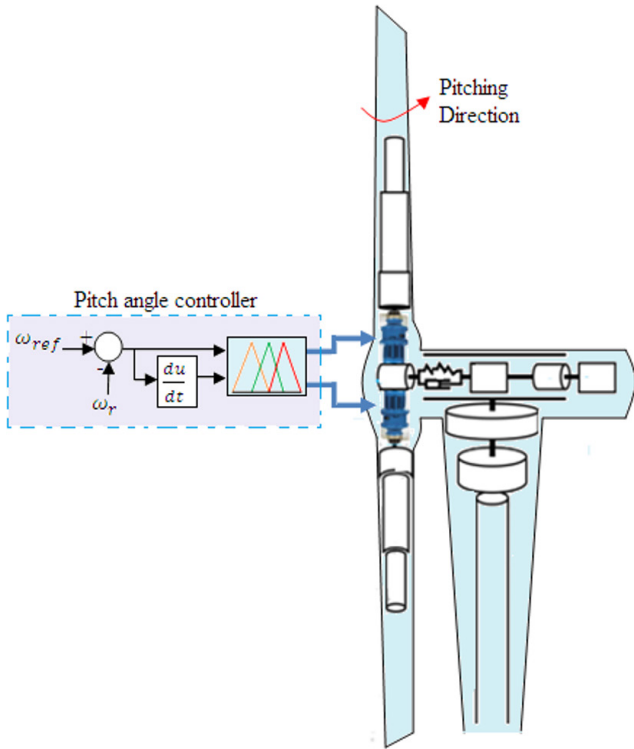


Fig. 5 Pitch angle control

its derivative for PVs and WECs systems are given in Eqs. (9) and (10):

$$\begin{cases} e_{PV}(k) = \frac{P_{PV}(k) - P_{PV}(k-1)}{V_{PV}(k) - V_{PV}(k-1)}, \\ de_{PV}(k) = e_{PV}(k) - e_{PV}(k-1) \end{cases} \quad (9)$$

$$\begin{cases} e_{WECs}(k) = \frac{P_{WECs}(k) - P_{WECs}(k-1)}{\omega(k) - \omega_r(k-1)} \\ de_{WECs}(k) = e_{WECs}(k) - e_{WECs}(k-1) \end{cases} \quad (10)$$

The membership function and rule table for the WECs system are given in Fig. 6 and Table 1. Fig. 7 shows the membership functions of e , de , and duty cycle for the PV controller when the base rule is given in Table 2. These memberships functions and base rules are utilized in the

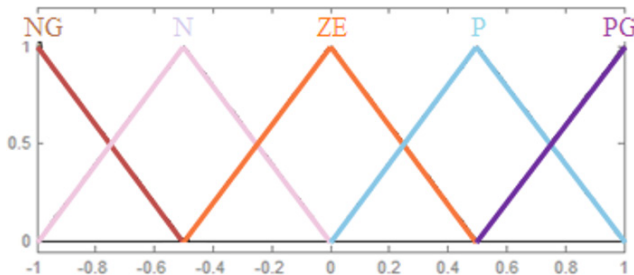
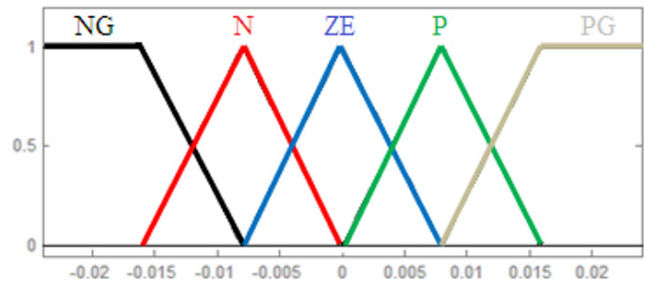


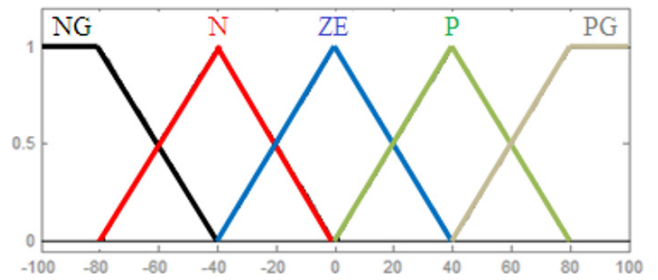
Fig. 6 Memberships functions of (e , de) and duty cycle for WECs and pitch angle controllers

Table 1 Basic rules for WECs controller

du	de					
	NG	N	Z	P	PG	
NG	Z	Z	PG	PG	PG	
N	Z	Z	P	P	P	
e	ZE	P	Z	Z	Z	N
P	N	P	N	Z	Z	
PG	NG	NG	NG	Z	Z	



(a)



(b)

Fig. 7 Membership functions of; (a) the error and its derivative (e , de); (b) duty cycle of the PV controller

Table 2 Rule bases for PVs controller

du	de					
	NG	N	ZE	P	PG	
NG	ZE	ZE	PG	PG	PG	
N	ZE	ZE	P	P	P	
e	ZE	P	ZE	ZE	ZE	N
P	N	P	N	ZE	ZE	
PG	NG	NG	NG	ZE	ZE	

system (b) as a common MPPT controller. The symbols PL, P, ZE, N, NL, mean positive, positive, zero, negative, and negative large, respectively.

3.6 Inverter control

The power produced by renewable energies is unstable which can negatively affect the operation of the electrical grid. Therefore, inverter control plays an important role in ensuring high power quality and keeping the DC voltage constant. Generally, the inverter control consists of three

essential parts which are the phase-locked loop (PLL), the DC-link voltage controller, and the currents controller. The voltage-oriented control (VOC) is applied to separate the active and reactive power control. Thus, dq reference rotation is done along with the grid voltage vector ($V_d = V$ and $V_q = 0$). Consequently, the powers injected into the grid (P_g, Q_g) will be controlled independently by I_d and I_q currents, respectively [6]. These powers are given in Eqs. (11) to (13) [23]:

$$\begin{cases} P_g = \frac{3}{2}V_d I_d \\ Q_g = -\frac{3}{2}V_d I_q \end{cases} \quad (11)$$

Considering inverter losses negligible, the active power can be e-written as this:

$$P_g = \frac{3}{2}V_d I_d = V_{DC} I_{DC} \quad (12)$$

The voltage control loop aims to maintain the DC voltage at a desired constant value. The reference value of the current (I_d^*) is estimated here by comparing the measured DC voltage to its reference value as detailed in Eq. (13):

$$I_d^* = \left(k_{d,p1} + \frac{k_{d,i1}}{s} \right) (V_{DC}^* - V_{DC}) \quad (13)$$

As given in Eq. (11), the reactive power can be controlled by the q -axis current (I_q), so, to satisfy the unity power factor the reactive power must be equal to zero, thus the imposed reference value of I_q current is zero. The grid voltages can be presented by the following function:

$$\begin{cases} V_{dinv} = V_d - L_f \frac{dI_d}{dt} - R_f I_d - \omega_s L_f I_q \\ V_{qinv} = V_q - L_f \frac{dI_q}{dt} - R_f I_q + \omega_s L_f I_d \end{cases} \quad (14)$$

Using PI regulators for current regulation, the reference voltages in Eq. (14) can be re-written as follows:

$$\begin{cases} V_{dinv}^* = V_d + \left(k_{d,p2} + \frac{k_{d,i2}}{s} \right) (I_d^* - I_d) - \omega_s L_f I_q \\ V_{qinv}^* = V_q + \left(k_{d,p2} + \frac{k_{d,i2}}{s} \right) (I_q^* - I_q) + \omega_s L_f I_d \end{cases} \quad (15)$$

where V_{dinv}, V_{qinv} are the output voltages of the inverter in (d,q) reference and V_d, V_q are the grid voltages in (d,q) reference, ω_s is the hegrid frequency, L_f and R_f are the inductance and the resistance of the RL filter.

The PLL is used to match the frequency of the inverter's output current with the grid. Moreover, in detail, an accurate phase-angle estimation is crucial in the control of energy flows and power factors [24]. The detailed inverter control is shown in Fig. 8.

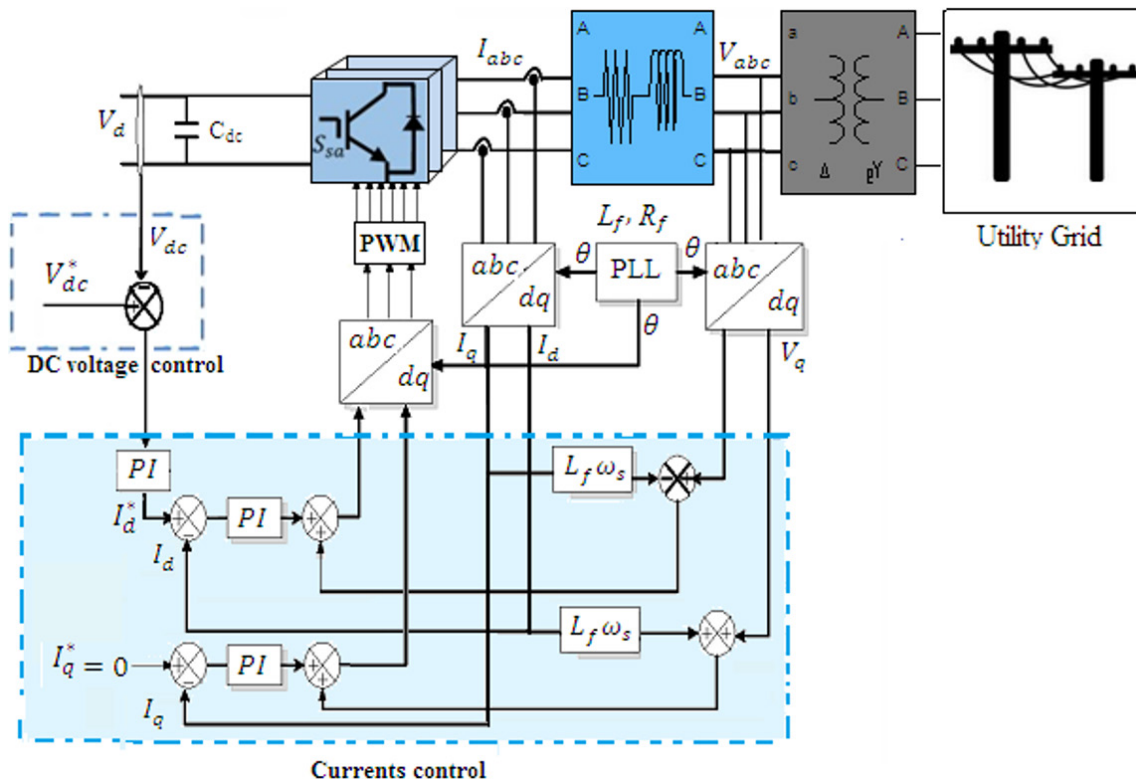


Fig. 8 Inverter control

4 Simulation results

The system simulated in this article consists of a photo-voltaic system supplying 25 kW and WECs composed of three turbines, each providing 8.5 kW. The Simulation parameters are given in Table 3.

Systems are simulated under MATLAB/Simulink [25] to verify the system performance under variations of metrological conditions and load demand (Figs. 9 to 11). The irradiance variation varies the PV current due to their linear relationship modeled in Eq. (1). Consequently, the PV output power varies automatically as it is in function of voltage and current ($P_{pv} = I_{pv} V_{pv}$). In the WECs system, the variation in wind speed varies directly with the

Table 3 Simulation parameters

PV module		PMSG	
Maximum power	200 W	Number of pole pairs	$p = 5$
Maximum current	8.21 A	Inductance	0.0082 H
Maximum voltage	32.9 V	Resistance	0.425 Ω
Cells in series	54	Frictional factor	0.001189 N m s/rad
Series resistance	0.2172 Ω	Inertia constant	0.01197 kg m ²

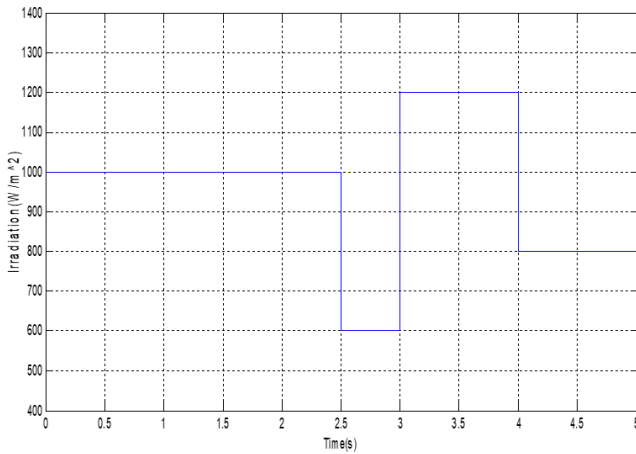


Fig. 9 Irradiation profile

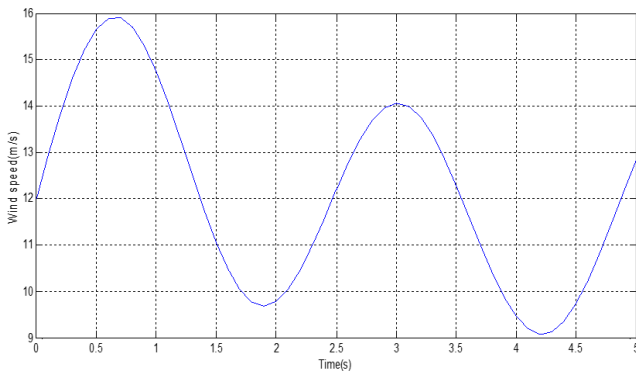


Fig. 10 Wind speed profile

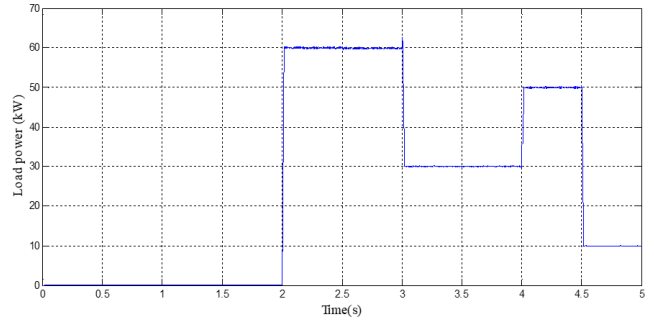


Fig. 11 Load power

WECs output power as is detailed in Eq. (2). As a result, the hybrid power varies instantaneously with the two conditions (sunlight irradiation and wind speed) proving the high efficiency of FLC control to tracks instantly the MPP of PVs and WECs while environmental conditions change. However, this power depends on the converter yield too. Each time the power passes through an electrical converter, it loses a part of its value due to the switching part. Therefore, the power of the first system is lower than the second, as in this system each subsystem passes through a DC/DC converter which means two losses are added in the PV system and the WECs system. In the second the total power passes via a single converter, which means that only one reduction is considered. As a result, the power of the using fewer converters (system (b)) is higher than the other which uses more (system (a)) as shown in Fig. 12. However, system (a) exhibits a faster response time of (0.5 s) than the second one due to the use of individual MPPT controllers. The reactive power of both systems is kept at zero value with a very negligible error which proves the efficiency of the control applied to guarantee the unity power factor.

The exchange of energy between the system and the grid is well controlled as shown in Fig. 13. In the ranges ((0–2 s), (3–4 s), and (4.5–5 s)), the hybrid power is more

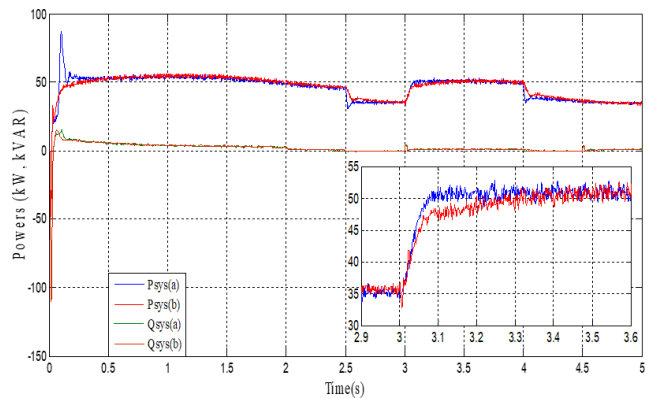


Fig. 12 Inverter powers of each system

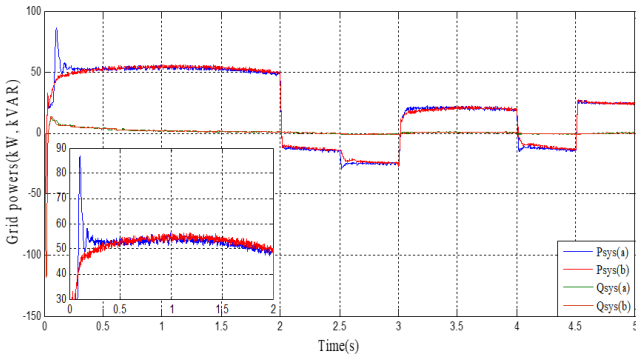


Fig. 13 Grid powers of each system

than the load requirement, so the surplus power is injected to the grid instantaneously. In ranges (2–3 s) and (4–4.5 s), the hybrid system is incapable of covering the load power, so the deficit power is recovered by the grid. When the reactive power is maintained at a zero value.

To remark on the difference between the two topologies, the subsystem simulation results are presented in Figs. 14 and 15. In system (b), the results show a very high oscillation, and the effect of climate changes of each system to another is remarked due to the use of single MPPT controller. This coupling effect appeared also in the rotational speed in 2.5 s, 3 s, and 4 s as presented in Fig. 16 which can damage the functionality of PMSG. This effect

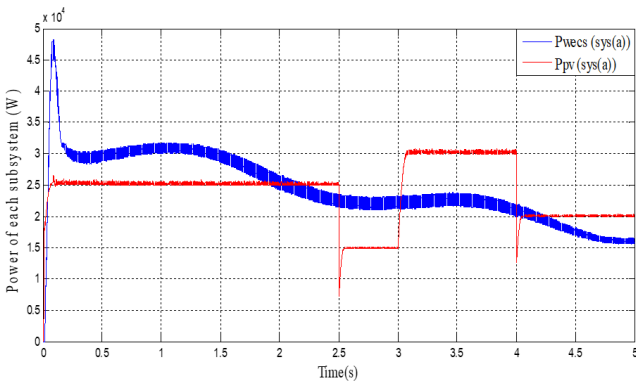


Fig. 14 Powers of subsystem (a)

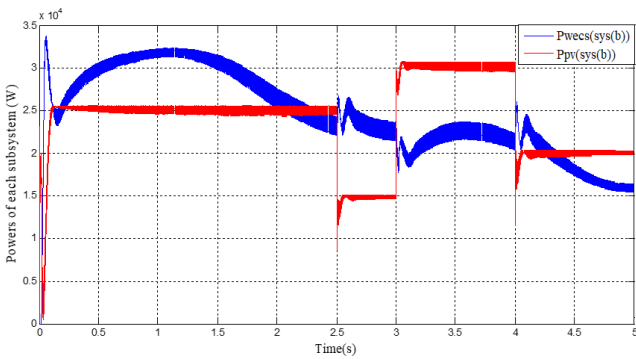


Fig. 15 Powers of the subsystem (b)

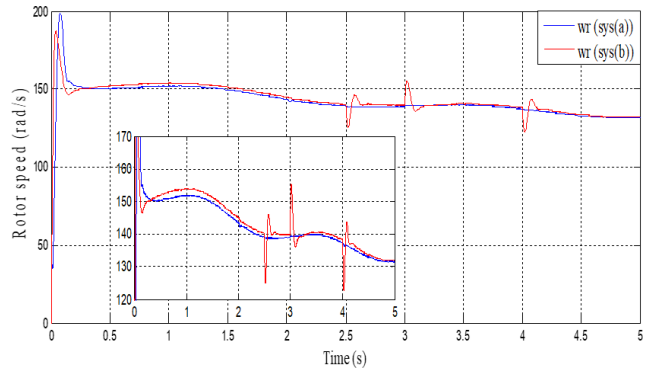


Fig. 16 Rotational speed

can degrade the operation of subsystems (chattering phenomena in the mechanical system). Contrary to system (a), the results of subsystems are very satisfactory without any ripples or coupling effect that proves the high performances of this system compared to the other one.

Fig. 17 shows the DC bus voltage which is kept constant (400 V) without any error regardless of the variations in irradiation and wind speed. The currents and voltages are below sinusoidal (Fig. 18). The total harmonic distortion (THD) of both systems are almost equal (3.24% and 3.29%) as shown in Fig. 19. The power factor remains unity, as shown in Fig. 20, proving the effectiveness of the applied control.

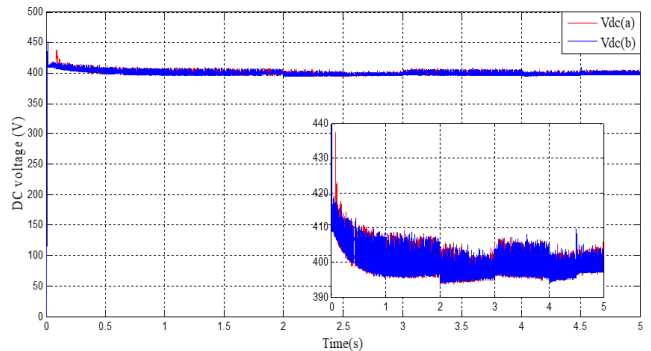


Fig. 17 DC voltage

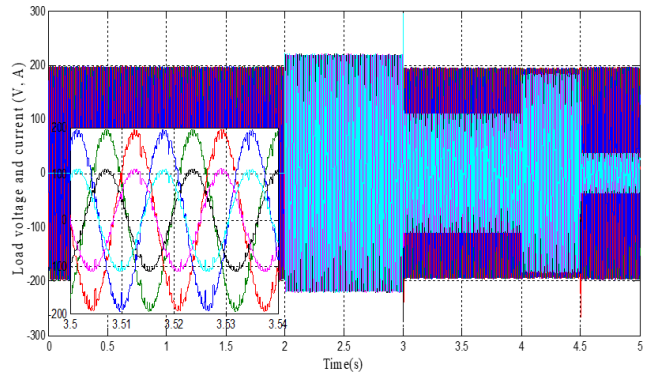


Fig. 18 Load voltage and current

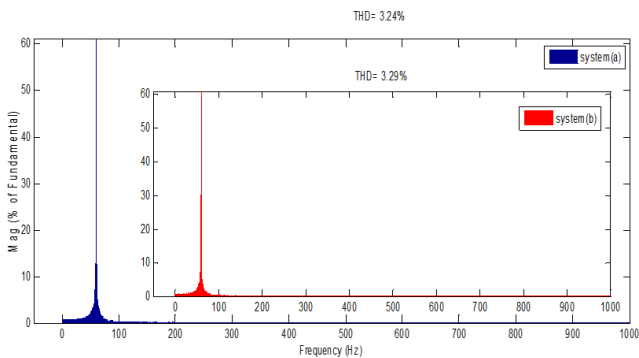


Fig. 19 Courant THD

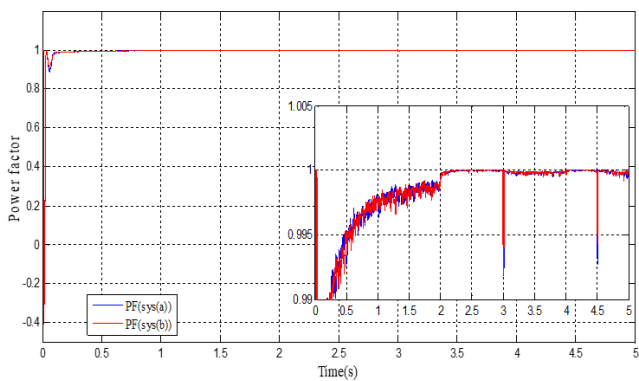


Fig. 20 Power factor

The system uses a common MPPT that minimizes the total number of converters, which means the reduction of the losses present at each converter. As a result, this system gives more energy than the other system (over 1 Kw) as shown in Table 4. However, due to the use of a single MPPT controller, this system showed a high dependency

References

- [1] Subudhi, B., Pradhan, R. "A New Adaptive Maximum Power Point Controller for a Photovoltaic System", *IEEE Transactions on Sustainable Energy*, 10(4), pp. 1625–1632, 2019. <https://doi.org/10.1109/TSTE.2018.2865753>
- [2] Adamo, F., Attivissimo, F., Di Nisio, A., Spadavecchia, M. "Characterization and Testing of a Tool for Photovoltaic Panel Modeling", *IEEE Transactions on Instrumentation and Measurement*, 60(5), pp. 1613–1622, 2011. <https://doi.org/10.1109/TIM.2011.2105051>
- [3] Kumar, K., Ramesh Babu, N., Prabhu, K. R. "Design and Analysis of RBFN-Based Single MPPT Controller for Hybrid Solar and Wind Energy System", *IEEE Access*, 5, pp. 15308–15317, 2017. <https://doi.org/10.1109/ACCESS.2017.2733555>
- [4] Ab-BelKhair, A., Rahebi, J., Abdulhamed Mohamed Nureddin, A. "A Study of Deep Neural Network Controller-Based Power Quality Improvement of Hybrid PV/Wind Systems by Using Smart Inverter", *International Journal of Photoenergy*, 2020(1), 8891469, 2020. <https://doi.org/10.1155/2020/8891469>
- [5] Rezvani, A., Esmaily, A., Etaati, H., Mohammadinodoushan, M. "Intelligent hybrid power generation system using new hybrid fuzzy-neural for photovoltaic system and RBFNSM for wind turbine in the grid-connected mode", *Frontiers in Energy*, 13(1), pp. 131–148, 2019. <https://doi.org/10.1007/s11708-017-0446-x>
- [6] Bouguerra, Z., Benfdila, A. "Comparative Study of Individual and Hybrid Renewable Energy Systems (Photovoltaic, Wind Energy and Hybridization). Controlled by Fuzzy Logic Control", *Journal of Engineering Science and Technology Review*, 14(5), pp. 180–186, 2021. <https://doi.org/10.25103/jestr.145.21>
- [7] Allani, M. Y., Riahi, J., Vergura, S., Mami, A. "FPGA-Based Controller for a Hybrid Grid-Connected PV/Wind/Battery Power System with AC Load", *Energies*, 14(8), 2108, 2021. <https://doi.org/10.3390/en14082108>

Table 4 Powers value of each system

Time (s)		2.3 s	2.7 s	3.5 s	4.7 s
System (a)	P	45.8	34.948	50.099	34.949
	Q	0.209	0.019	0.724	0.37
System (b)	P	46.627	36.398	50.641	35.134
	Q	0.195	0.024	0.808	0.35

between the two subsystems such as the appearance of the variation effect between the PVs and WECs systems with a very high oscillation compared to the system (a).

5 Conclusion

A comparative study between two hybridization topologies of PVs and WECs systems supplying 50 kW is studied in this work. In the first topology, PVs and WECs are connected to the DC bus through several rectifiers controlled by individual MPPTs. In the second design, both systems are connected to a common rectifier. The performances of these topologies are tested under varying weather conditions (wind speed, irradiation) and load requirements. The simulation results prove that; the high efficiency of different controls applied, FLC control varies instantly with the weather variations, and the inverter control guarantees a unity power factor. The performance of the individual MPPT is superior to the common MPPT, even though the latter gives more power (over 1 kW), but it may degrade the operation of the subsystems, especially in the mechanical wind conversion system (chattering phenomenon) due to the occurrence of the weather change effect in each subsystem.

- [8] Shanthi, P., Uma, G., Keerthana, M. S. "Effective power transfer scheme for a grid-connected hybrid wind/photovoltaic system", *IET Renewable Power Generation*, 11(7), pp. 1005–1017, 2017.
<https://doi.org/10.1049/iet-rpg.2016.0592>
- [9] Abouddrar, I., El Hani, S., Heyine, M. S., Naseri, N. "Dynamic Modeling and Robust Control by ADRC of Grid-Connected Hybrid PV-Wind Energy Conversion System", *Mathematical Problems in Engineering*, 2019(1), 8362921, 2019.
<https://doi.org/10.1155/2019/8362921>
- [10] Nzoundja Fapi, C. B., Tchakounté, H., Ndje, M., Wira, P., Kamta, M. "Extraction of the Global Maximum Power for PV System under PSC Using an Improved PSO Technique", *Periodica Polytechnica Electrical Engineering and Computer Science*, 68(1), pp. 64–73, 2024.
<https://doi.org/10.3311/PPee.22254>
- [11] Latkova, M., Bahernik, M., Hoger, M., Bracnik, P. "FSM Model of a Simple Photovoltaic System", *Advances in Electrical and Electronic Engineering*, 13(3), pp. 230–235, 2015.
<https://doi.org/10.15598/aeec.v13i3.1411>
- [12] Vu, P.-V., Nago, V.-T., Do, V.-D., Truong, D.-N., Huynh, T.-T., Do, T. D. "Robust MPPT Observer-Based Control System for Wind Energy Conversion System With Uncertainties and Disturbance", *IEEE Access*, 9, pp. 96466–96477, 2021.
<https://doi.org/10.1109/ACCESS.2021.3094819>
- [13] Bouguerra, Z. "Comparative study between PI, FLC, SMC, and Fuzzy sliding mode controllers of DFIG wind turbine", *Journal of Renewable Energies*, 26(2), pp. 209–223, 2023.
<https://doi.org/10.54966/jreen.v26i2.1146>
- [14] Jabal Laafou, A., Ait Madi, A., Addaim, A., Intidam, A. "Dynamic Modeling and Improved Control of a Grid-Connected DFIG Used in Wind Energy Conversion Systems", *Mathematical Problems in Engineering*, 2020(1), 1651648, 2020.
<https://doi.org/10.1155/2020/1651648>
- [15] Pradhan, S., Singh, B., Panigrahi, B. K., Murshid, S. "A Composite Sliding Mode Controller for Wind Power Extraction in Remotely Located Solar PV–Wind Hybrid System", *IEEE Transactions on Industrial Electronics*, 66(7), pp. 5321–5331, 2019.
<https://doi.org/10.1109/TIE.2018.2868009>
- [16] Howlader, A. M., Senjyu, T., Saber, A. Y. "An Integrated Power Smoothing Control for a Grid-Interactive Wind Farm Considering Wake Effects", *IEEE Systems Journal*, 9(3), pp. 954–965, 2015.
<https://doi.org/10.1109/JSYST.2014.2374311>
- [17] Prince, M. K. K., Arif, M. T., Gargoom, A., Oo, A. M. T., Haque, M. E. "Modeling, Parameter Measurement, and Control of PMSG-based Grid-connected Wind Energy Conversion System", *Journal of Modern Power Systems and Clean Energy*, 9(5), pp. 1054–1065, 2021.
<https://doi.org/10.35833/MPCE.2020.000601>
- [18] Zhao, Y., Wei, C., Zhang, Z., Qiao, W. "A Review on Position/Speed Sensorless Control for Permanent-Magnet Synchronous Machine-Based Wind Energy Conversion Systems", *IEEE Journal of Emerging and Selected Topics in Power Electronics*, 1(4), pp. 203–216, 2013.
<https://doi.org/10.1109/JESTPE.2013.2280572>
- [19] Osman, A. M., Alsokhry, F. "Sliding Mode Control for Grid Integration of Wind Power System Based on Direct Drive PMSG", *IEEE Access*, 10, pp. 26567–26579, 2022.
<https://doi.org/10.1109/ACCESS.2022.3157311>
- [20] Haq, I. U., Khan, Q., Khan, I., Akmeiliawati, R., Nisar, K. S., Khan, I. "Maximum Power Extraction Strategy for Variable Speed Wind Turbine System via Neuro-Adaptive Generalized Global Sliding Mode Controller", *IEEE Access*, 8, pp. 128536–128547, 2020.
<https://doi.org/10.1109/ACCESS.2020.2966053>
- [21] Majout, B., Bossoufi, B., Bouderbala, M., Masud, M., Al-Amri, J. F., Taoussi, M., El Mahfoud, M., Motahhir, S., Karim, M. "Improvement of PMSG-Based Wind Energy Conversion System Using Developed Sliding Mode Control", *Energies*, 15(5), 1625, 2022.
<https://doi.org/10.3390/en15051625>
- [22] Van, T. L., Nguyen, T. H., Lee, D.-C. "Advanced Pitch Angle Control Based on Fuzzy Logic for Variable-Speed Wind Turbine Systems", *IEEE Transactions on Energy Conversion*, 30(2), pp. 578–587, 2015.
<https://doi.org/10.1109/TEC.2014.2379293>
- [23] Ahmed, M., Harbi, I., Kennel, R., Rodríguez, J., Abdelrahem, M. "Evaluation of the Main Control Strategies for Grid-Connected PV Systems", *Sustainability*, 14(18), 11142, 2022.
<https://doi.org/10.3390/su141811142>
- [24] Freijedo, F. D., Yepes, A. G., Lopez, Ó., Fernandez-Comesana, P., Doval-Gandoy, J. "An Optimized Implementation of Phase Locked Loops for Grid Applications", *IEEE Transactions on Instrumentation and Measurement*, 60(9), pp. 3110–3119, 2011.
<https://doi.org/10.1109/TIM.2011.2122550>
- [25] The Mathworks "MATLAB, (R2021b)", [computer program] Available at: <https://matlab.mathworks.com> [Accessed: 17 September 2020]